

Electromagnetic Analysis of Wireless Power Transfer System with Improved Absorbing Boundary Conditions

K. Sugahara

Kindai University, Japan

Abstract— The performance of the Improved Absorbing Boundary Conditions (IABC) is studied when applied to wireless power transfer (WPT) systems. The IABC is one of the approximated techniques to solve the unbounded electromagnetic problems. It was recently proposed to solve quasi-static problems and extended to the high frequencies. Non-radiative WPT based on the magnetic resonance and near-field coupling of two-loop resonators was first reported by Tesla and nowadays, it has attracted interest from industry and academic researchers. The frequency used in non-radiative WPT systems are rather low and therefore, high frequency electromagnetic techniques e.g., radiation boundary conditions and PML are not applicable to analyze the WPT systems. In this manuscript, the advantages of the IABC is discussed.

1. INTRODUCTION

Huge numbers of research paper have been published during the past 40 years on the open boundary technique for electromagnetic analysis. It is a long-standing topic which is still discussed in the recent literature [6–8]. The perfect matching layers are artificial absorbing layers which is a major technique in high frequency electromagnetics. That was first proposed by Berenger [2] in 1994 and Complex Frequency Shifted (CFS) PML was proposed afterwards [4] which was also applicable to evanescent waves. There are also some discussions to modify the PML technique to extend to the static problems [3, 5].

Artificial layers in low-frequency application were proposed in 2013 [6, 7]. The Improved Asymptotic Boundary Conditions (IABC) utilizes approximated unbounded space as series of isotropic spherical shells so as to emulate open boundaries without the need for additional code to any finite element solver. This idea was extended to formulate the high frequency version of Improved Absorbing Boundary Conditions (IABC) by the author [8]. In this manuscript, the advantages of the IABC are discussed, when applied to wireless power transfer (WPT) systems.

2. IMPROVED ABSORBING BOUNDARY CONDITION

Figure 1 shows a schematic image of the third-order improvised absorbing condition. The region of interest is inside the inner boundary and the surrounding outer shells work as absorbers. The outermost boundary is a PEC.

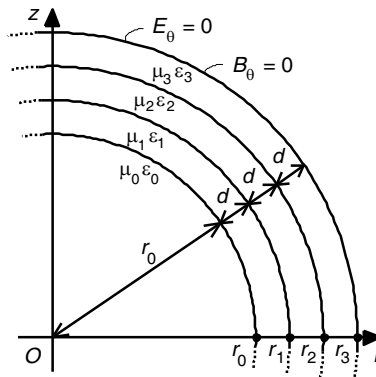


Figure 1: Schematic image of the three-layer improvised absorbing boundary condition.

The formulation of the IABC is discussed in [8]. By solving the equation in [8], appropriate electric and magnetic constants for the IABC layers are obtained given in Table 1. N corresponds to the order of the IABC which is equivalent to the number of layers. The size of the analysis domain is 0.5 m. The frequency is 13.56 MHz. The thickness of each IABC layer is 0.05 m.

Table 1: Electric constants of the IABC layers.

N	1st layer	2nd layer	3rd layer	4th layer	5th layer
1	$\mu_1 = 10.2594 - 0.0281j$ $\varepsilon_1 = 0.1806 - 0.0005j$				
2	$\mu_1 = 0.3472 + 0.0009j$ $\varepsilon_1 = 2.6708 + 0.0123j$	$\mu_2 = 20.8827 - 0.1848j$ $\varepsilon_2 = 0.1182 - 0.0006j$			
3	$\mu_1 = 1.7025 - 0.0049j$ $\varepsilon_1 = 0.6249 - 0.0027j$	$\mu_2 = 0.2021 + 0.0011j$ $\varepsilon_2 = 5.1602 + 0.0530j$	$\mu_3 = 31.3801 - 0.6916j$ $\varepsilon_3 = 0.1059 - 0.0009j$		
4	$\mu_1 = 0.7969 + 0.0018j$ $\varepsilon_1 = 1.2273 + 0.0039j$	$\mu_2 = 2.9451 - 0.0207j$ $\varepsilon_2 = 0.3827 - 0.0034j$	$\mu_3 = 0.1601 + 0.0013j$ $\varepsilon_3 = 7.5767 + 0.1211j$	$\mu_4 = 43.0158 - 1.9854j$ $\varepsilon_4 = 0.1008 - 0.0011j$	
5	$\mu_1 = 1.0880 - 0.0015j$ $\varepsilon_1 = 0.9262 - 0.0015j$	$\mu_2 = 0.5596 + 0.0036j$ $\varepsilon_2 = 1.7409 + 0.0136j$	$\mu_3 = 4.3479 - 0.0511j$ $\varepsilon_3 = 0.2748 - 0.0029j$	$\mu_4 = 0.1422 + 0.0018j$ $\varepsilon_4 = 9.9639 + 0.2056j$	$\mu_5 = 56.5685 - 5.0367j$ $\varepsilon_5 = 0.0969 - 0.0009j$

3. WIRELESS POWER TRANSFER SYSTEM

Figure 2 shows an example of the WPT system discussed in this manuscript. It has two resonators opposed each other whose resonance frequency is designed to be 13.56 MHz. Those two resonators are open-ended and made of copper. Both the receiver and transmitter are one-turn coils. Diameters of the resonators are 380 mm and the gap in-between is 200 mm.

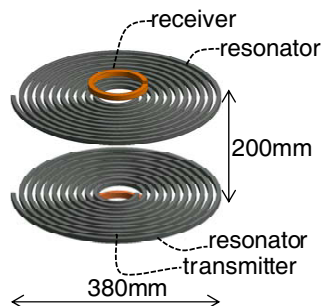


Figure 2: Schematic image of the WPT system.

Figure 3 shows a frequency-dependence of the power transmission. The lower peak (13.6 MHz) corresponds to the even mode and the higher (14.7 MHz) to the odd mode. Figure 4 shows each peak with different boundary conditions. Black lines correspond to the result with the CFS-PML [4], green ones with the PML [2], red ones with the radiation boundary conditions [1] with different size of the analysis domain, and blue ones with the three, four, and five-layer IABCs. The result with three-layer, four-layer, and five-layer IABCs are almost identical whereas the results with different sizes of the radiation boundary conditions significantly differ with each other.

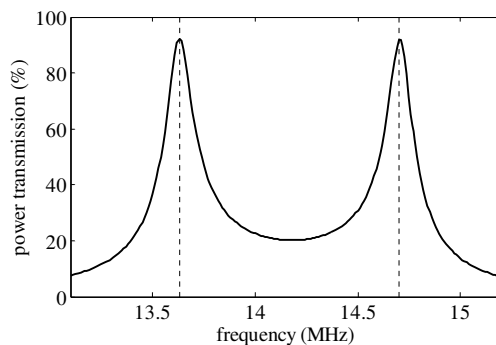


Figure 3: Frequency-dependence of the power transmission.

Figure 5 shows the electromagnetic field distributions obtained by the FEM with the three-layer IABC and reconstructed from the surface. (a)–(d) correspond to even-modes and (e)–(h) to odd-modes. Figure 6 shows the electromagnetic field distributions obtained by the FEM with the

radiation boundary conditions and reconstructed from the surface. (a)–(d) correspond to even-modes and (e)–(h) to odd-modes.

As shown in Figures 5 and 6, the reconstructed fields inside the analysis domain is almost zeros with the three-layer IABC whereas non-zero with the radiation boundary conditions. This indicates that reflections from the boundary are small when the IABC is employed, however significant reflections can be observed with the radiation boundary conditions. Table 2 shows dominant multipoles of the even and odd modes. The highest multipoles is the sextupole, therefore, three-layers is assumed to be enough.

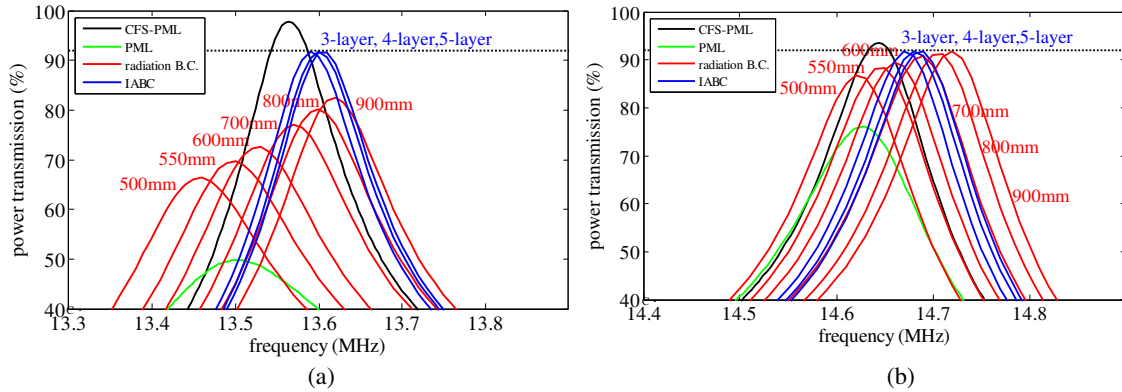


Figure 4: (a) even-mode peak of the power transmission, and (b) odd-mode peak with different types of the boundary conditions.

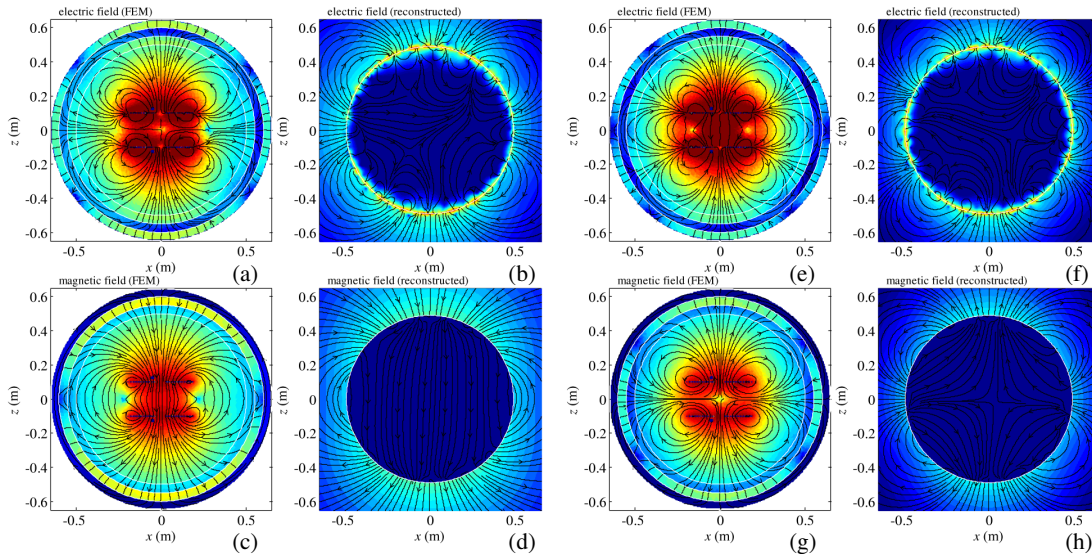


Figure 5: Contour plots and flux lines of (a) even-mode electric field obtained by the FEM with the three-layer IABC, (b) even-mode electric field reconstructed from the surface, (c) even-mode magnetic field obtained by the FEM with the three-layer IABC, (d) even-mode electric field reconstructed from the surface, (e) odd-mode electric field obtained by the FEM with the three-layer IABC, (f) odd-mode electric field reconstructed from the surface, (g) odd-mode magnetic field obtained by the FEM with the three-layer IABC, and (h) odd-mode electric field reconstructed from the surface.

Table 2: Dominant multipoles of each mode.

	even mode	odd mode
electric field	quadrupole	sextupole
magnetic field	dipole	quadrupole

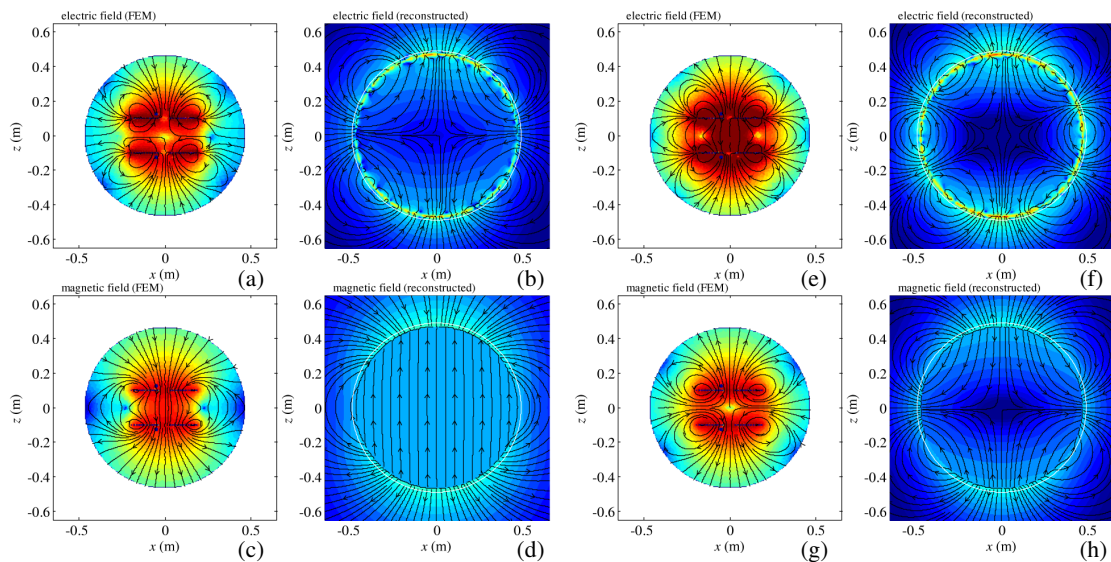


Figure 6: Contour plots and flux lines of (a) even-mode electric field obtained by the FEM with the radiation boundary condition, (b) even-mode electric field reconstructed from the surface, (c) even-mode magnetic field obtained by the FEM with the radiation boundary condition, (d) even-mode magnetic field reconstructed from the surface, (e) odd-mode electric field obtained by the FEM with the radiation boundary condition, (f) odd-mode electric field reconstructed from the surface, (g) odd-mode magnetic field obtained by the FEM with the radiation boundary condition, and (h) odd-mode magnetic field reconstructed from the surface.

4. CONCLUSION

In this manuscript, the performance of the Improved Absorbing Boundary Conditions is studied when applied to the Wireless Power Transfer systems. Since the coupling between electric and magnetic fields is important in the non-radiative WPT system, electromagnetic field solver must be employed. However, the frequencies used in the non-radiative WPT systems are rather small and the conventional absorbing boundary conditions are not applicable. Examples in this manuscript indicate that the IABC works as good absorbers.

REFERENCES

1. Mittra, R. and O. Ramahi, "Absorbing boundary conditions for the direct solution of partial-differential equations arising in electromagnetic scattering problems," *PIER 2: Finite Element and Finite Difference Methods in Electromagnetic Scattering*, M. A. Morgan, Ed., Chapter 4, Elsevier, New York, 1990.
2. Berenger, J. P., "A perfect matched layer for the absorption of electromagnetic waves," *J. Comp. Phys.*, Vol. 114, 185–200, 1994.
3. Alfonzetti, S., G. Borz, and N. Salerno, "Some considerations about the perfectly matched layer for static fields," *COMPEL*, Vol. 18, 337–347, 1999.
4. Roden, J. A. and S. D. Gedney, "Convolutional PML (CPML): An efficient FDTD implementation of the CFS-PML for arbitrary media," *Microwave and Optical Technology Lett.*, Vol. 27, No. 5, 334–338, 2000.
5. Dedek, L., J. Dedkova, and J. Valsa, "Optimization of perfectly matched layer for Laplace's equation," *IEEE Trans. Magn.*, Vol. 38, 501–504, 2002.
6. Meeker, D., "Improved open boundary conditions for magnetic finite elements," *IEEE Trans. Magn.*, Vol. 49, 5243–5247, 2013.
7. Meeker, D., "Improved asymptotic boundary conditions for electrostatic finite elements," *IEEE Trans. Magn.*, Vol. 50, No. 6, 7400609, 2014.
8. Sugahara, K., "Improved absorbing boundary conditions for three-dimensional electromagnetic finite elements," *2015 International Conference on Electromagnetics in Advanced Applications (ICEAA)*, 1094–1097, 2015.